Available online at www.sciencedirect.com

ScienceDirect

Ceramics International 40 (2014) 13033–13039

CERAMICS INTERNATIONAL

www.elsevier.com/locate/ceramint

Influence of dilution effect on the electrochemical performance of integrated $0.5Li(Mn_{1.5}Ni_{0.5})O_4$. $0.5(Li_2MnO_3–Li(Mn_{0.5}Ni_{0.5})O_2)$ cathodes

In Hyung Choi[a], Jae Min Choi[a], Yun Ju Hwang[b], Vanchiappan Aravindan[d], Yun Sung Lee[e,*], Kee Suk Nahm[a,b,c,**]

[a]Department of Energy Storage and Conversion Engineering, Chonbuk National University, Jeon-ju 561-756, Republic of Korea
[b]R&D Education Center for Fuel Cell Materials & Systems, Chonbuk National University, Jeon-ju 561-756, Republic of Korea
[c]School of Chemical Engineering, Chonbuk National University, Jeon-ju 561-756, Republic of Korea
[d]Energy Research Institute@NTU (ERI@N), Nanyang Technological University, Research Techno Plaza, 50 Nanyang Drive, Singapore 637553, Singapore
[e]Faculty of Applied Chemical Engineering, Chonnam National University, Gwang-ju 500-757, Republic of Korea

Received 28 March 2014; received in revised form 24 April 2014; accepted 30 April 2014
Available online 9 May 2014

Abstract

We report the influence of dilution effect on the synthesis and electrochemical profiles of integrated spinel–layered $0.5Li(Mn_{1.5}Ni_{0.5})O_4$. $0.5(Li_2MnO_3–Li(Mn_{0.5}Ni_{0.5})O_2$ cathodes prepared by scalable continuous stirred tank reactor (CSTR). Apparently, the dilution of chelating agent or precursor solutions leads to the formation of unavoidable impurity phases. However, the presence of such impurity traces certainly improves the electrochemical stability of such spinel–layered integrated electrodes. In addition, influence of operating potential is also investigated and it was found that 2.4–4.8 V vs. Li is the optimal condition to yield high capacity and high performance cathode material.

Keywords: Integrated cathodes; Layered–spinel; Li-ion battery

1. Introduction

Zero emission transportation applications such as hybrid electric vehicles (HEV) and electric vehicles (EV) requires high energy density Li-ion power packs. Nevertheless, the construction of high energy Li-ion batteries (LIB) completely depends on the utilization of high capacity and high voltage cathodes [1]. Unfortunately, the commercially available existing layered type $LiCoO_2$ is limited to 0.5 mol of Li ($\sim$137 mAh g^{-1}) only [2]. On the other hand, native spinel ($LiMn_2O_4$) and olivine phosphates ($LiMPO_4$, M=Fe, Mn and Co) and its derivatives are exhibiting the practical capacity less than 150 mA h g^{-1} [3]. In addition, V_2O_5 and orthosilicates (Li_2MSiO_4, M=Fe, Mn and Co) are also considered as promising cathode with high theoretical limitations however irreversible structural change and inferior electrochemical profiles of former and latter counterparts renders them as "show-case" cathodes [3–6]. Mixture of two cathodes are also one of the solutions to achieve desirable high capacity and high power cathodes for LIB applications which has been successfully adopted for the Sony's NEXLION configuration ($LiCoO_2$+Li(Co-Ni-Mn)O_2) [1]. These kinds of integrated cathodes can be prepared easily by a conventional synthesis route or simple mechanical/manual mixing of two electrode counterparts. Apart from the capacity point of view, eco-friendliness and cost-effectiveness cannot be ruled out for such cathodes. In this line, Fe and Mn based electrodes are the choice, but richness in the oxidation states, higher operating

*Corresponding author. Tel./fax: +82 62 530 1904.
**Corresponding author at: Department of Energy Storage and Conversion Engineering, Chonbuk National University, Jeon-ju 561-756, Republic of Korea. Tel.: +82 63 270 2311; fax: +82 63 270 3909.
E-mail addresses: leeys@chonnam.ac.kr (Y. Sung Lee), nahmks@jbnu.ac.kr (K. Suk Nahm).

http://dx.doi.org/10.1016/j.ceramint.2014.04.167
0272-8842/

potential and high stability makes Mn based materials attractive than Fe, although having the issue of Jahn–Teller distortion [7].

Among the Mn based candidates, layered type Li_2MnO_3 (analogue of α-$NaFeO_2$) exhibits high theoretical capacity ~459 mA h g^{-1} for the removal of two moles of Li [8–10]. Unfortunately, Li_2MnO_3 is electrochemically inactive, hence the removal of Li is not plausible, because the transition metal Mn is already in the 4+ state and it is impossible to oxidize further in to 5+ state [8]. Hitherto, there are four main reasons believed for the electrochemical activity of such layered type Li_2MnO_3, (i) Oxidation of Mn^{3+} associated with oxygen deficiency ($Li_2MnO_{3-\delta}$), (ii) Removal of lithium accompanied by oxygen loss (Li_2O), (iii) Oxidation of electrolyte solution and subsequent exchange of H^+ for Li^+ and (iv) Oxidation of other transition-metal elements (observed only in the solid-solutions) [11,12]. For the preparation of integrated electrodes, the solid solution plays a vital role to determine the energy density i.e. operating potential. Generally, the integrated electrodes comprising the formula xLi_2MnO_3. $(1-x)LiMO_2$, M=Ni, Co, M for "layered–layered" and x Li_2MnO_3. $(1-x)$ LiM_2O_4, M=Ni, Co, Mn for "layered–spinel", in which Li_2MnO_3 translates better structural and electrochemical stabilities irrespective of either layered $LiMO_2$ or spinel LiM_2O_4 components for wider operating potential [13,14]. In addition to the native layered and spinel counterparts, the metal substituted derivatives were also investigated to improve the cycleability and electrochemical profiles. Amongst, layered–layered electrodes are found promising in terms of capacity, but the net energy density is more or less equal to that of layered $LiCoO_2$ only. Hence, the research focus is directed to layered–spinel integrated cathodes, since Ni-substituted spinel ($LiMn_2O_4$) exhibits the higher redox potential than native compound [15]. In this line we made an attempt to explore the possibility of using high voltage and high capacity integrated electrodes ($0.5Li(Mn_{1.5}Ni_{0.5})O_4$. $0.5(Li_2MnO_3–Li(Mn_{0.5}Ni_{0.5})O_2)$) by a carbonate co-precipitation technique. The extensive structural and electrochemical profiles were evaluated and described in detail.

2. Experimental

The solid-solution was composed of integrated spinel–layered type x $Li(Mn_{1.5}Ni_{0.5})O_4$. $(1-x)$ $[Li_2MnO_3–Li(Mn_{0.5}Ni_{0.5})O_2]$, where $x=0.5$ was prepared by the carbonate co-precipitation technique in a continuous stirred tank reactor (CSTR). All the analytical grade starting materials such as Li_2CO_3, Na_2CO_3, $MnSO_4$, $NiSO_4$, and NH_4OH were procured and used as such. The Na_2CO_3 solution was used as the chelating agent to control the precipitation of the precursor. For the preparation of layered–spinel integrated materials precursor, transition metal (Mn:Ni) ratio was fixed to 3:1. Several synthesis parameters were used to tailor the $Mn_{0.75}Ni_{0.25}CO_3$ precursor. The resultant $Mn_{0.75}Ni_{0.25}CO_3$ was filtered, washed well with distilled water and dried at 100 °C for 12 h in air atmosphere. The desired product was yielded after reacting with appropriate amount of Li_2CO_3 in solid-state reaction at 650 °C for 5 h, and then fired at 900 °C for 12 h in air.

Structural properties were analyzed by X-ray diffraction (XRD) measurements using Rint 1000 Regaku, Japan equipped with Cu Kα radiation. Morphological features of the powders were observed by field emission scanning electron microscopy. The electrochemical characterizations were performed in CR2032 coin-cell configuration. The composite electrodes were formulated with accurately weighed 20 mg of active material, 3 mg of conductive additive (Ketzen black) and 3 mg of Teflonized acetylene black (TAB-2) using ethanol and pressed over 150 mm^2 nickel mesh and dried at 160 °C for 4 h in vacuum oven. Test cells were fabricated with metallic lithium which was separated by porous polypropylene separator (Celgard 3401) under Ar filled Glove box. 1 M $LiPF_6$ ethylene carbonate (EC)/di-methyl carbonate (DMC) (1:1 v/v) was used as electrolyte solution. The galvanostatic charge–discharge studies were performed between 2 and 4.9 V vs. Li at current density of 0.1 mA cm^{-2} (0.05C) under ambient temperature conditions.

3. Results and discussion

Influence of dilution of the transition metal and chelating agent was on the synthesis of mixed carbonate studied. Precursor $Mn_{0.75}Ni_{0.25}CO_3$ has been prepared under various conditions such as inclusion of NH_4OH solution (P1), large amount of chelating agent usage (P2), diluting the chelating agent and without diluting transition metal counterparts (P3 and P4), dilution of both transition metal solution and chelating agent (P5 and P6) in CSTR with 150–400 rpm. Irrespective of the synthesis conditions, the precipitation of mixed transition metal carbonate was obtained. Fig. 1 shows the powder XRD patterns of $Mn_{0.75}Ni_{0.25}CO_3$ precursor prepared under various conditions according to Table 1. A trace amount of NiOOH is noted which is clearly evident from the XRD reflections (peak observed at ~11°) along with $MnCO_3$ content. The prominent reflection at ~31° ensures the crystallinity of the prepared mixed carbonate [16]. This clearly suggests that the dilution of precursor or chelating agent did

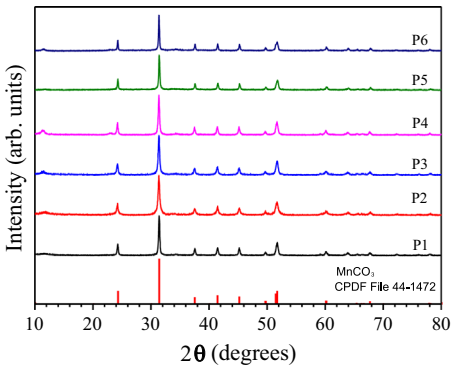

Fig. 1. Powder X-ray diffraction pattern of $Mn_{0.75}Ni_{0.25}CO_3$ prepared under various conditions according to the parameters presented in Table 1.

not influence the structural properties of the precursor. Morphological features of the $Mn_{0.75}Ni_{0.25}CO_3$ were analyzed by FE-SEM and are shown in Fig. 2. Apparent to note that all the resultant $Mn_{0.75}Ni_{0.25}CO_3$ powders exhibited the spherical shaped morphology, although with slight variation in the particulate shape. The breaking of the spherical shaped morphology is also noted which is mainly associated with the high speed rotation of the blade in the CSTR. Then, the $Mn_{0.75}Ni_{0.25}CO_3$ powders were manually ground with appropriate amount of Li_2CO_3 to yield the desired integrated layered–spinel phase compound by solid-state reaction.

Table 1
$0.5Li(Mn_{1.5}Ni_{0.5})O_4$–$0.5[Li_2MnO_3$–$Li(Mn_{0.5}Ni_{0.5})O_2]$ were obtained under various conditions. All the concentrations are in milliliter (ml).

Sample	1.5 M $MnSO_4$	0.5 M $NiSO_4$	D.I. water	2 M Na_2CO_3	1 M NH_4OH	D.I. water
P1	250	250	0	250	250	0
P2	250	250	0	500	0	0
P3	250	250	0	250	0	250
P4	250	250	0	500	0	500
P5	250	250	500	250	0	250
P6	250	250	500	500	0	500

XRD pattern of layered–spinel $0.5Li(Mn_{1.5}Ni_{0.5})O_4$–$0.5[Li_2MnO_3$–$Li(Mn_{0.5}Ni_{0.5})O_2]$ powder is shown in Fig. 3. All the XRD patterns clearly showed the strong reflections which were composed of layered, spinel and superstructure, for example the appearance of small peaks between 20° and 25° indicates the characteristic of Li_2MnO_3 superstructure [17,18]. The Li_2MnO_3 phase is indexed according to the monoclinic structure C2/*m* space group in which [0 0 1] closed packed plane is coincident with [0 0 3] plane. Generally, the superstructure formation is caused from the short-range ordering between Li-ions and transition metal atoms in the transition metal slab. In the present case, a clear separation of superstructure is noted which suggests the dominant characteristic of layered type Li_2MnO_3. Apart from the dilution, a basic

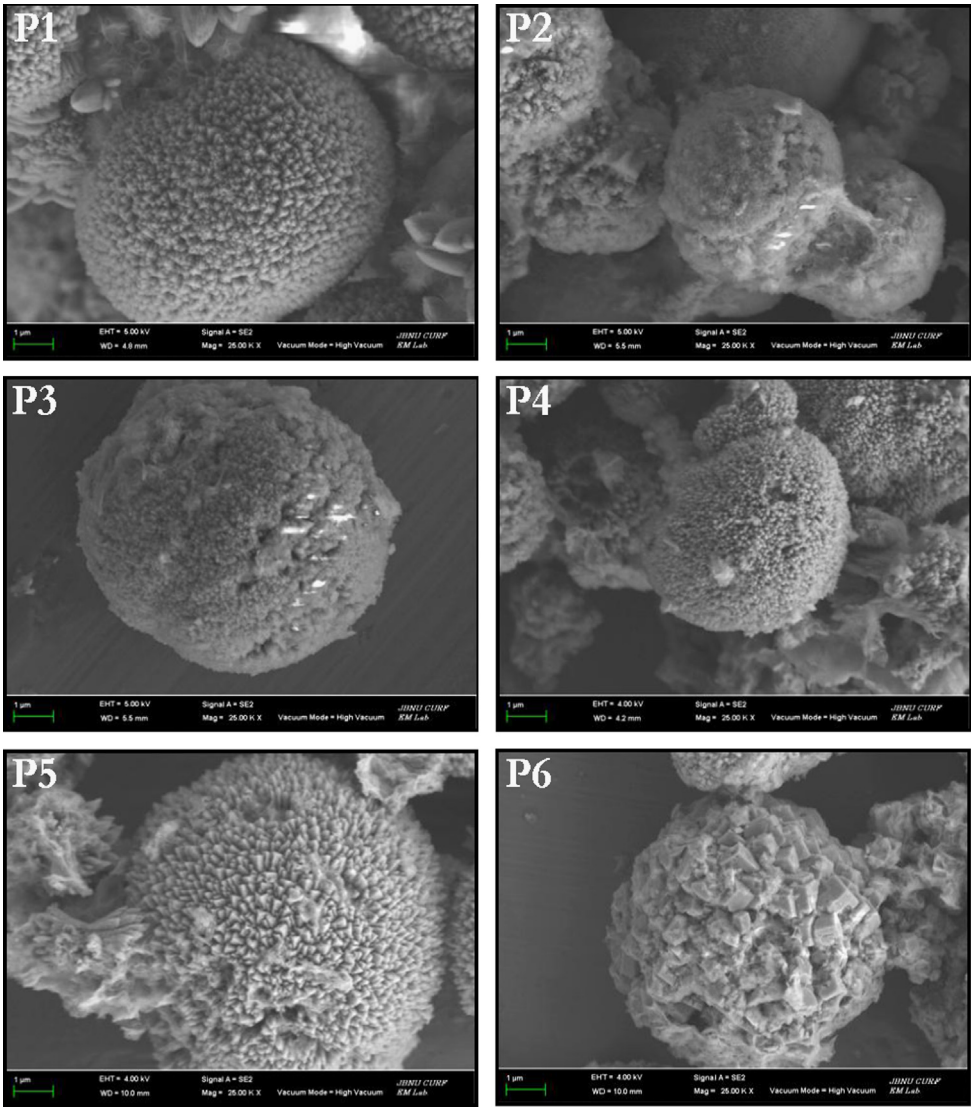

Fig. 2. FE-SEM pictures of $Mn_{0.75}Ni_{0.25}CO_3$ prepared under various conditions according to the parameters presented in Table 1.

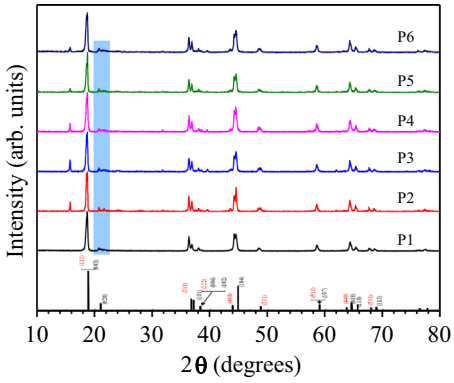

Fig. 3. XRD patterns of $0.5Li(Mn_{1.5}Ni_{0.5})O_4$–$0.5[Li_2MnO_3$–$Li(Mn_{0.5}Ni_{0.5})O_2]$ prepared under various conditions according to the parameters presented in Table 1. Red and black colored indexing belongs to the spinel and layered structures, respectively. The highlighted region belongs to the characteristics of Li_2MnO_3 superstructure. (For interpretation of the references to color in this figure legend, the reader is referred to the web version of this article.)

condition is necessary to yield a single phase materials, which is clearly observed from the XRD reflections, for example a trace amount of the unknown impurity phase is observed for all the cases (P2 – P6), except NH_4OH treated one (P1). Presence of spinel phase is clearly identified from the existence of the peak at $2\theta = \sim 37^o$ and $\sim 44^o$ which corresponds to the (3 1 1) and (4 0 0) planes, respectively. On the other hand, not much variation in the spherical shaped morphology is noted compared to the mixed carbonate precursors which is clearly supported from the FE-SEM pictures (Fig. 4).

The electrochemical profiles of layered–spinel $0.5Li(Mn_{1.5}Ni_{0.5})O_4.0.5[Li_2MnO_3$–$Li(Mn_{0.5}Ni_{0.5})O_2]$ were evaluated between 2 and 4.9 V vs. Li at current density of 0.1 mA cm^{-2} (0.05C rate) under ambient temperature conditions (Fig. 5). The first charge curve is entirely different than rest of the charge curves. During charging, a sharp increase in potential from open circuit voltage to ~4.5 V vs. Li corresponds to the removal of Li from the $Li(Mn_{0.5}Ni_{0.5})O_2$ lattice by single phase reaction and it is reversible as well.

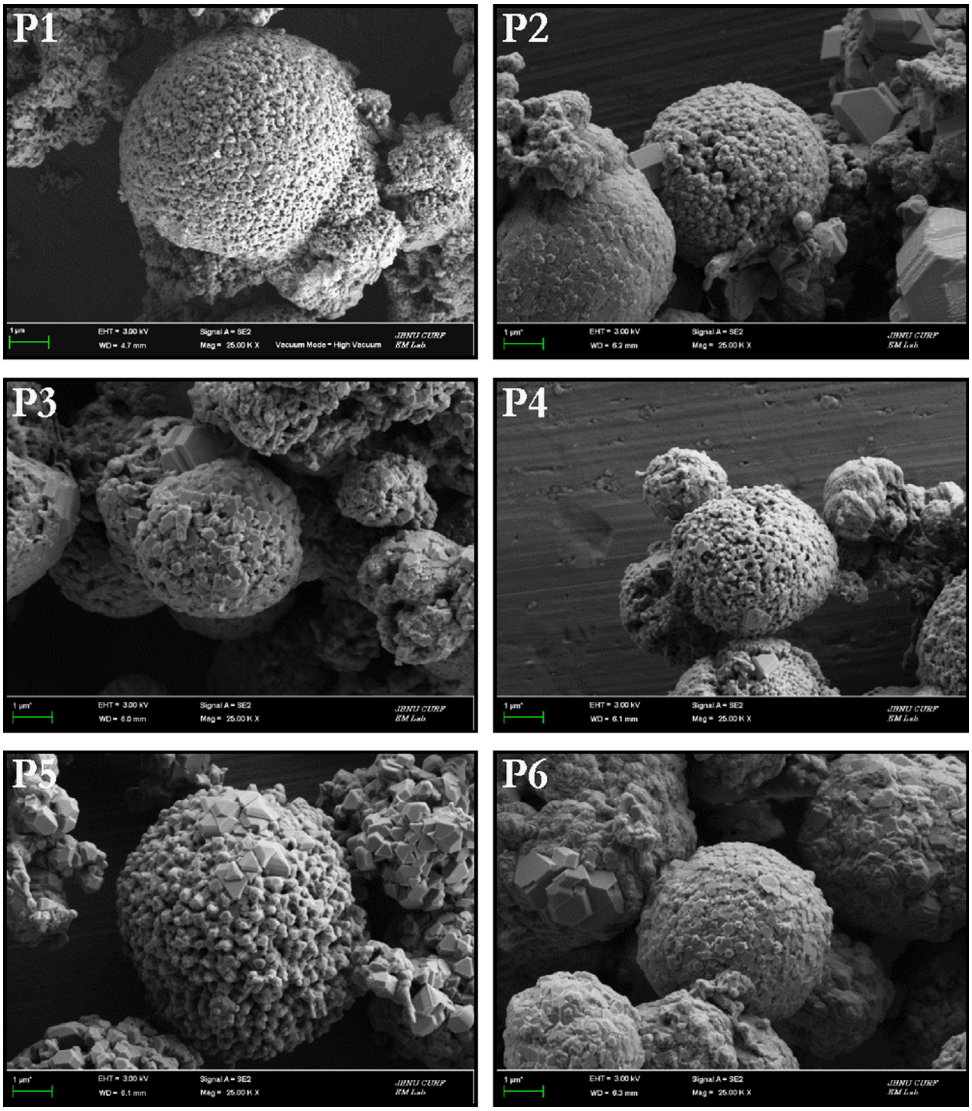

Fig. 4. FE-SEM pictures of $0.5Li(Mn_{1.5}Ni_{0.5})O_4$–$0.5[Li_2MnO_3$–$Li(Mn_{0.5}Ni_{0.5})O_2]$ prepared under various conditions according to the parameters presented in Table 1.

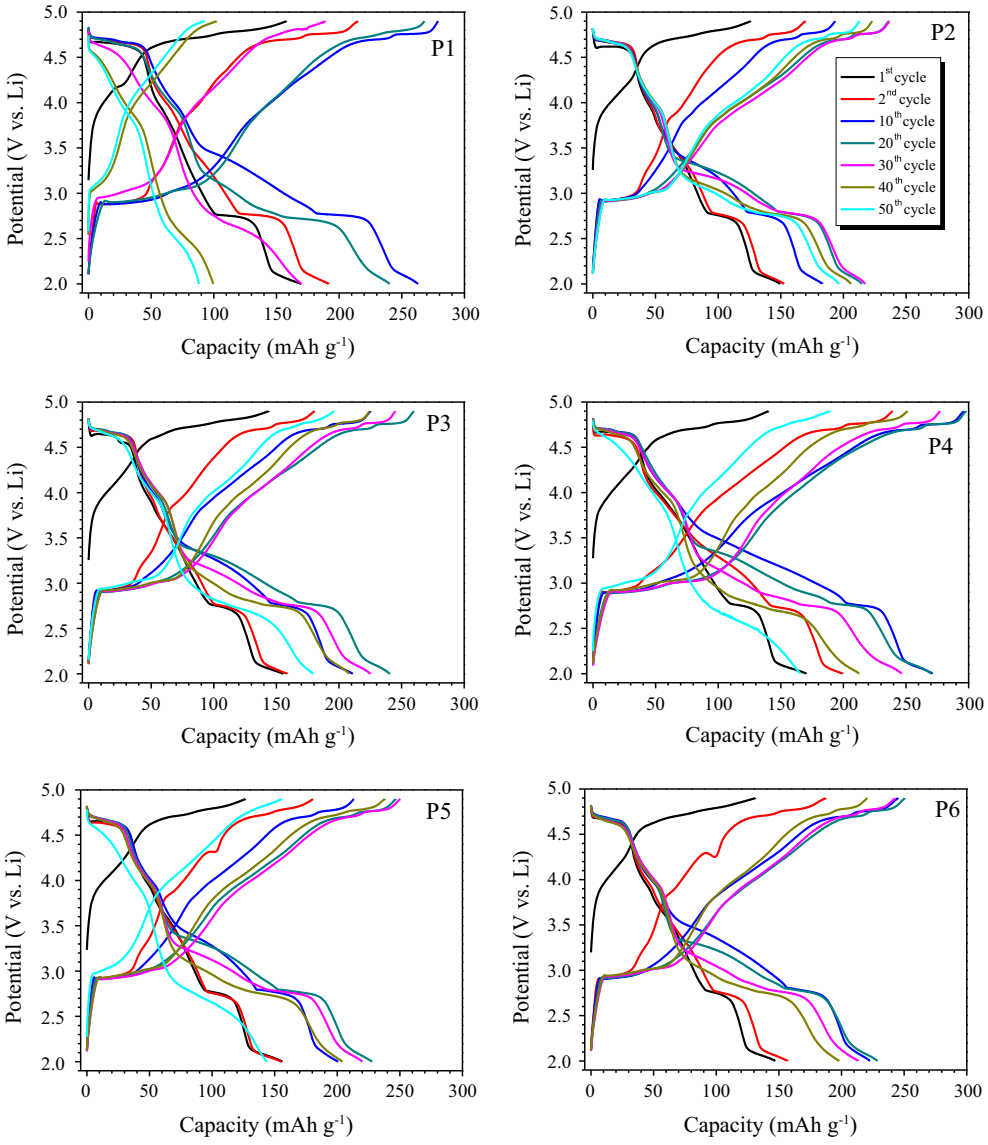

Fig. 5. Galvanostatic charge–discharge profiles of integrated spinel–layered 0.5 $Li(Mn_{1.5}Ni_{0.5})O_4$–0.5[Li_2MnO_3–$Li(Mn_{0.5}Ni_{0.5})O_2$] electrodes cycled between 2 and 4.9 V vs. Li at current density of 0.1 mA cm^{-2}.

The presence of slopping region above ~4.5 V vs. Li corresponds to the removal of Li and oxygen (net removal of Li_2O) and associated activation of layered Li_2MnO_3 ($Li_2MnO_{3-\delta}$) which is an irreversible reaction. Unlike that of the charging process, several reactions are noted during the discharge reaction. A small plateau around ~4.7 V vs. Li corresponds to the reversible Li-insertion into tetrahedral sites i.e. reduction of $Ni^{4+/2+}$ in spinel component ($Li(Mn_{1.5}Ni_{0.5})O_4$) [19]. The slopping region between ~4.5 and 2.7 V vs. Li corresponds to the contribution of layered type counterparts such as $Li_2MnO_{3-\delta}$ and $Li(Mn_{0.5}Ni_{0.5})O_2$ i.e. redox reaction of $Ni^{3+/2+}$ and partially $Mn^{4+/3+}$. The small plateau around ~2.7 V vs. Li is attributed to the reversible Li-insertion in to octahedral sites of spinel phase $Li(Mn_{1.5}Ni_{0.5})O_4$ in two-phase reaction mechanism i.e. reduction of $Mn^{4+/2+}$ [20,21]. The cell (P1) delivered the reversible capacity of ~170 mA h g^{-1} whereas other diluted samples present the reversible capacity of

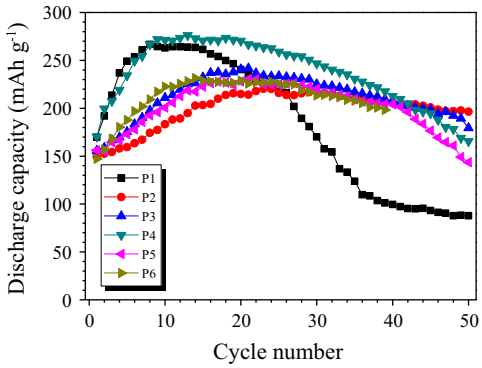

Fig. 6. Cycling profiles of integrated spinel–layered 0.5$Li(Mn_{1.5}Ni_{0.5})O_4$–0.5 [Li_2MnO_3–$Li(Mn_{0.5}Ni_{0.5})O_2$] electrodes cycled between 2 and 4.9 V vs. Li at current density of 0.1 mA cm^{-2}.

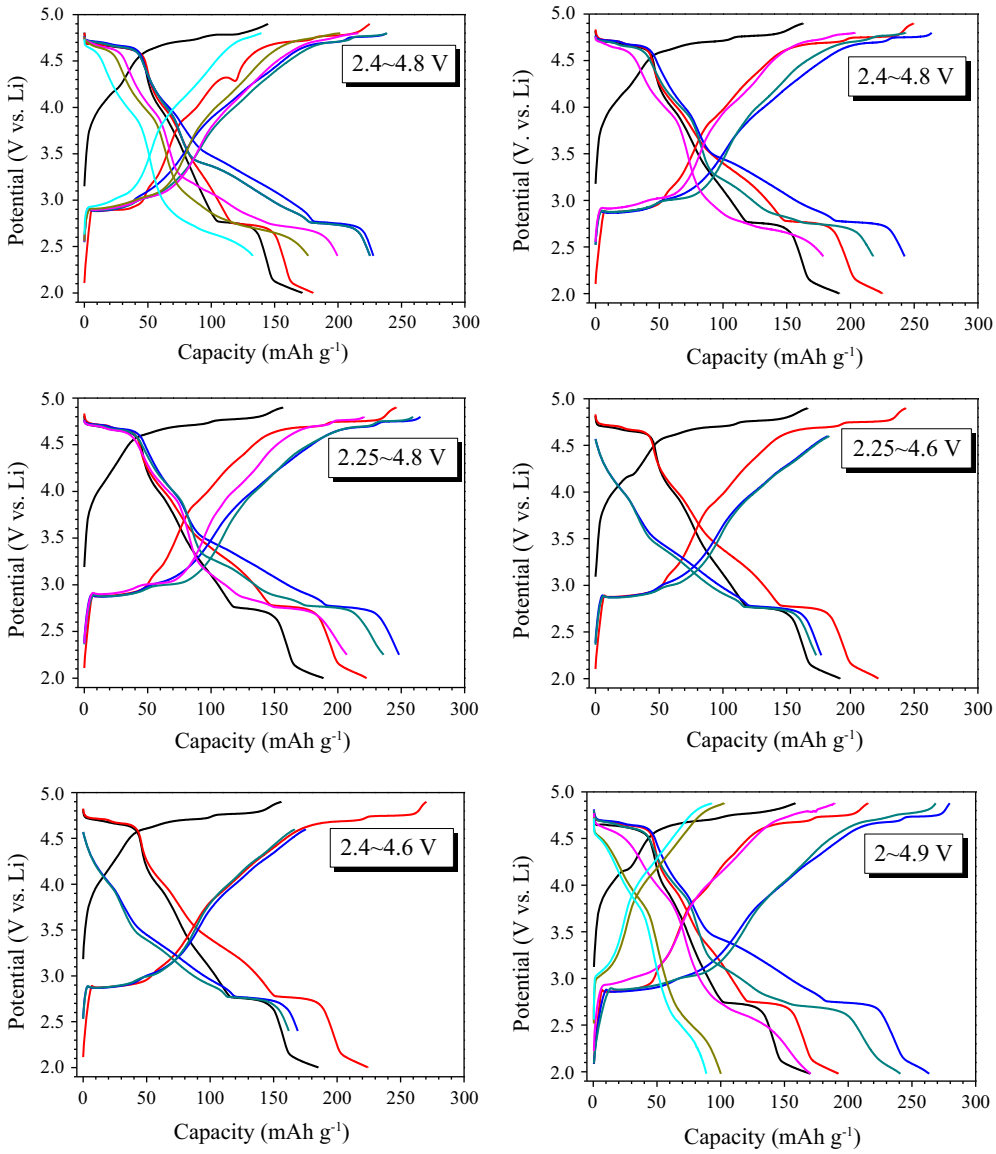

Fig. 7. Galvanostatic charge–discharge profiles of integrated spinel–layered $0.5Li(Mn_{1.5}Ni_{0.5})O_4$–$0.5[Li_2MnO_3$–$Li(Mn_{0.5}Ni_{0.5})O_2]$ electrodes cycled at current density of 0.1 mA cm^{-2} with various cut-off potentials.

$\sim$150 mA h g^{-1} only under the same current density, except P4 which exhibits $\sim$170 mA h g^{-1}. Irrespective of the layered–spinel integrated electrodes, increasing capacity profiles are noted for all the cases. Such increasing capacity profiles are common for the case of Li_2MnO_3 based cathodes, which is mainly due to the slower participation of the active material in the electrochemical reaction because of the presence of Mn^{4+} ions. Plot of discharge capacity vs. cycle number is depicted in Fig. 6. All the materials show the increasing capacity profile upon cycling, which is mainly attributed to the slower participation of the active materials. Unfortunately, after certain number of cycles (10–20 cycles) the decrease in capacity trends is noted. This decrease in capacity trends is mainly because of the cubic–tetragonal transformation occurring in the spinel counterpart which leads to structural instability. Moreover, the partial reduction of Mn^{4+} in to Mn^{3+} reduction in layered part and reversible insertion at $\sim$2.7 V vs. Li (reduction of Mn^{4+} in to Mn^{3+}) leads to the presence of Mn^{3+} ion, which is also having the problem of Jahn–Teller distortion. As a consequence, decrease in capacity profiles is noted for all the materials. Interestingly, except P1 all the materials rendered good electrochemical stability, we believe such stability is mainly because of the unknown impurity. But, our aim is to prepare the phase pure electrodes with improved electrochemical activity.

Then, we evaluated the influence of cut-off potential to improve the electrochemical profiles of phase pure spinel–layered integrated electrodes (P1) under the same current density of 0.1 mA cm^{-2} and is shown in Figs. 7 and 8. All the cases, first two cycles are performed between 2 and 4.9 V vs. Li to activate the layered electrode Li_2MnO_3. Apparent to note that, improved capacity retention is noted between 2.4 and 4.8 V vs. Li when compared to 2 and 4.9 V vs. Li, for example the integrated spinel–layered delivered the capacity of $\sim$135 and $\sim$85 mA h g^{-1} for former and latter cut-off potentials respectively. However, the maximum

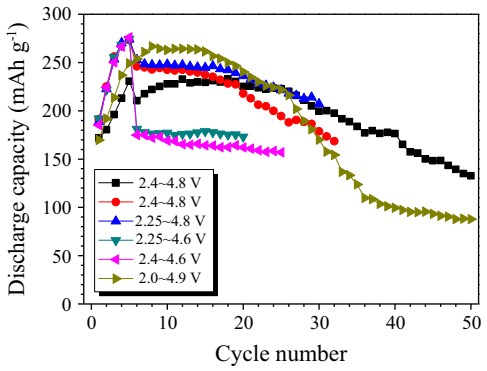

Fig. 8. Cycling profiles of integrated spinel–layered $0.5Li(Mn_{1.5}Ni_{0.5})O_4$–$0.5[Li_2MnO_3$–$Li(Mn_{0.5}Ni_{0.5})O_2]$ electrodes cycled at current density of 0.1 mA cm^{-2} with various cut-off potentials.

deliverable capacity has been suppressed. This clearly suggests that the 2.4–4.8 V vs. Li is the optimal condition to yield high capacity cathode active material. Further studies are in progress to improve the capacity fading during cycling.

4. Conclusion

We studied the dilution effect of integrated spinel–layered $0.5Li(Mn_{1.5}Ni_{0.5})O_4$–$0.5[Li_2MnO_3$–$Li(Mn_{0.5}Ni_{0.5})O_2]$ cathodes synthesized via CSTR. Present results clearly reveal the dilution of either chelating agent or precursor which results in the formation of unwanted impurity phase along with the desired phase. Further, influence of testing potential also validated to improve the electrochemical stability during cycling. Amongst, testing window 2.4–4.8 V vs. Li was found optimum to yield high capacity and high performance cathode. This preliminary result strongly encourage to develop such integrated spinel–layered cathodes to fabricate high energy density Li-ion power packs for HEV and EV applications.

Acknowledgments

This research was supported by Basic Science Research Program through the National Research Foundation of Korea (NRF) funded by the Ministry of Education (No. 2013R1A1A2012656) and was also supported by research funds of Chonbuk National University in 2011.

References

[1] V. Aravindan, J. Gnanaraj, Y.-S. Lee, S. Madhavi, $LiMnPO_4$ – a next generation cathode material for lithium-ion batteries, J. Mater. Chem. A 1 (2013) 3518–3539.
[2] Y. Nishi, The development of lithium ion secondary batteries, Chem. Rec. 1 (2001) 406–413.
[3] C. Masquelier, L. Croguennec, Polyanionic (phosphates, silicates, sulfates) frameworks as electrode materials for rechargeable Li (or Na) batteries, Chem. Rev. 113 (2013) 6552–6591.
[4] V. Aravindan, K. Karthikeyan, K.S. Kang, W.S. Yoon, W.S. Kim, Y.S. Lee, Influence of carbon towards improved lithium storage properties of Li_2MnSiO_4 cathodes, J. Mater. Chem. 21 (2011) 2470–2475.
[5] V. Aravindan, K. Karthikeyan, S. Ravi, S. Amaresh, W. Kim, Y. Lee, Adipic acid assisted sol–gel synthesis of Li_2MnSiO_4 nanoparticles with improved lithium storage properties, J. Mater. Chem. 20 (2010) 7340–7343.
[6] V. Aravindan, K. Karthikeyan, J. Lee, S. Madhavi, Y. Lee, Synthesis and improved electrochemical properties of Li_2MnSiO_4 cathodes, J. Phys. D 44 (2011) 152001.
[7] S. Okada, J.-i. Yamaki, Iron-based cathodes/anodes for Li-ion and post Li-ion batteries, J. Ind. Eng. Chem. 10 (2004) 1104–1113.
[8] A.D. Robertson, P.G. Bruce, The origin of electrochemical activity in Li_2MnO_3, Chem. Commun. 23 (2002) 2790–2791.
[9] A.D. Robertson, P.G. Bruce, Mechanism of electrochemical activity in Li_2MnO_3, Chem. Mater. 15 (2003) 1984–1992.
[10] P. Kalyani, S. Chitra, T. Mohan, S. Gopukumar, Lithium métal rechargeable cells using Li_2MnO_3 as the positive electrode, J. Power Sources 80 (1999) 103–106.
[11] K. Kubota, T. Kaneko, M. Hirayama, M. Yonemura, Y. Imanari, K. Nakane, R. Kanno, Direct synthesis of oxygen-deficient Li_2MnO_{3-x} for high capacity lithium battery electrodes, J. Power Sources 216 (2012) 249–255.
[12] Y. Koyama, I. Tanaka, M. Nagao, R. Kanno, First-principles study on lithium removal from Li_2MnO_3, J. Power Sources 189 (2009) 798–801.
[13] M.M. Thackeray, S.-H. Kang, C.S. Johnson, J.T. Vaughey, R. Benedek, S.A. Hackney, , Li_2MnO_3-stabilized $LiMO_2$ (M=Mn, Ni, Co) electrodes for lithium-ion batteries, J. Mater. Chem. 17 (2007) 3112–3125.
[14] N. Yabuuchi, K. Yoshii, S.-T. Myung, I. Nakai, S. Komaba, Detailed studies of a high-capacity electrode material for rechargeable batteries, $Li_2MnO_3-LiCo_{1/3}Ni_{1/3}Mn_{1/3}O_2$, J. Am. Chem. Soc. 133 (2011) 4404–4419.
[15] J. Cabana, S.-H. Kang, C.S. Johnson, M.M. Thackeray, C.P. Grey, Structural and electrochemical characterization of composite layered–spinel electrodes containing Ni and Mn for Li-Ion batteries, J.Electrochem. Soc. 156 (2009) A730–A736.
[16] D. Wang, I. Belharouak, G.M. Koenig, G. Zhou, K. Amine, Growth mechanism of $Ni_{0.3}Mn_{0.7}CO_3$ precursor for high capacity Li-ion battery cathodes, J. Mater. Chem. 21 (2011) 9290–9295.
[17] K. Karthikeyan, S. Amaresh, G.W. Lee, V. Aravindan, H. Kim, K.S. Kang, W.S. Kim, Y.S. Lee, Electrochemical performance of cobalt free, $Li_{1.2}(Mn_{0.32}Ni_{0.32}Fe_{0.16})O_2$ cathodes for lithium batteries, Electrochim. Acta 68 (2012) 246–253.
[18] K. Karthikeyan, S. Amaresh, V. Aravindan, W.S. Kim, K.W. Nam, X.Q. Yang, Y.S. Lee, $Li(Mn_{1/3}Ni_{1/3}Fe_{1/3})O_2$–polyaniline hybrids as cathode active material with ultra-fast charge–discharge capability for lithium batteries, J. Power Sources 232 (2013) 240–245.
[19] M.C. Kim, K.-W. Nam, E. Hu, X.-Q. Yang, H. Kim, K. Kang, V. Aravindan, W.-S. Kim, Y.-S. Lee, Sol–gel synthesis of aliovalent vanadium-doped $LiNi_{0.5}Mn_{1.5}O_4$ cathodes with excellent performance at high temperatures, ChemSusChem 7 (2014) 829–834.
[20] S. Jayaraman, V. Aravindan, P. Suresh Kumar, W.C. Ling, S. Ramakrishna, S. Madhavi, Synthesis of porous $LiMn_2O_4$ hollow nanofibers by electrospinning with extraordinary lithium storage properties, Chem. Commun. 49 (2013) 6677–6679.
[21] F. Jiao, J. Bao, A.H. Hill, P.G. Bruce, Synthesis of ordered mesoporous Li–Mn–O spinel as a positive electrode for rechargeable lithium batteries, Angew. Chem. Int. Ed. 47 (2008) 9711–9716.